(5) A. Karipides and T. S. Piper, *J. Chem. Phys.*, **40**, 674 (1964).
(6) R. Kuroda and Y. Saito, *Bull. Chem. Soc. Jpn.*, **49**, 433 (1976).
(7) R. R. Judkins and D. J. Royer, *Inorg. Chem.*, **13**, 945 (1974).
(8) B. Bosnich, "Fundamental Aspects and Recent Developments in Optical Dispersion and Circular Dichrosim", Ciardelli and Salvatory, Ed., Heyden and Son Ltd., London, 1973, Chapter 3.7.
(9) R. D. Gillard, S. H. Laurie, D. C. Price, D. A. Phipps, and C. F. Weich, *J. Chem. Soc., Dalton Trans.*, 1385 (1974).
(10) K. R. Butler and M. R. Snow, *J. Chem. Soc., Dalton Trans.*, 251 (1976).
(11) J. Ferguson, C. J. Hawkins, N. A. P. Kane-Maguire, and H. Lip, *Inorg. Chem.*, **8**, 771 (1969).
(12) P. G. Beddoe, M. J. Harding, S. F. Mason, and P. G. Peart, *Chem. Commun.*, 1283 (1971).
(13) R. Kuroda, J. Fujita, and Y. Saito, *Chem. Lett.*, 225 (1975).
(14) Single-crystal CD spectra of eight cobalt(III) and chromium(III) complexes have been reported: ref 6, 15, 43; H. P. Jensen and F. Galsbøl, *Inorg. Chem.*, **16**, 1294 (1977).
(15) A. J. McCaffery, S. F. Mason, and R. E. Ballard, *J. Chem. Soc.*, 2883 (1965).
(16) T. S. Piper and R. L. Carlin, *J. Chem. Phys.*, **35**, 1809 (1961).
(17) S. Yamada and R. Tsuchida, *Bull. Chem. Soc. Jpn.*, **33**, 98 (1960).
(18) R. Dingle and C. J. Ballhausen, *K. Dan. Vidensk. Selsk., Mat.-Fys. Medd.*, **35**, No. 12 (1967).
(19) R. B. Von Dreele and R. C. Fay, *J. Am. Chem. Soc.*, **93**, 4936 (1971).
(20) M. R. Snow, *Acta Crystallogr., Sect. B*, **30**, 1850 (1974).
(21) G. J. Kruger and E. C. Reynhardt, *Acta Crystallogr., Sect. B*, **30**, 822 (1974).
(22) D. Karipides and W. C. Fernelius, *Inorg. Synth.*, **8**, 56 (1963).
(23) P. Ray and N. K. Dutt, *J. Indian Chem. Soc.*, **16**, 621 (1939).
(24) P. Ray and N. K. Dutt, *J. Indian Chem. Soc.*, **18**, 289 (1941).
(25) B. E. Bryant and W. C. Fernelius, *Inorg. Synth.*, **5**, 188 (1957).
(26) "International Tables for X-Ray Crystallography", Vol. 1, Kynoch Press, Birmingham, England, 1965, p 99.
(27) J. A. Bertrand, E. Fujita, and P. G. Eller, *Inorg. Chem.*, **13**, 2067 (1974).
(28) P. W. R. Clearfield, R. J. Doedens, and J. A. Ibers, *Inorg. Chem.*, **6**, 197 (1967).
(29) D. T. Cromer and J. T. Waber, *Acta Crystallogr.*, **18**, 104 (1965).
(30) R. F. Stewart, E. R. Davidson, and W. T. Simpson, *J. Chem. Phys.*, **42**, 3175 (1965).
(31) D. T. Cromer, *Acta Crystallogr.*, **18**, 17 (1965).
(32) N. C. Moucharafieh, Ph.D. Thesis, Georgia Institute of Technology, 1976.
(33) E. I. Stiefel and G. F. Brown, *Inorg. Chem.*, **11**, 434 (1972).
(34) K. R. Dymock and G. J. Palenik, *Inorg. Chem.*, **14**, 1220 (1975).
(35) A. Avdeef and J. P. Fackler, Jr., *Inorg. Chem.*, **14**, 2002 (1975).
(36) K. Michelsen, *Acta Chem. Scand.*, **19**, 1175 (1965).
(37) T. S. Piper, *J. Chem. Phys.*, **35**, 1240 (1961).
(38) D. J. Royer, *Inorg. Chem.*, **17**, 512 (1978).
(39) S. H. Lin, *J. Chem. Phys.*, **55**, 3546 (1971).
(40) C. O. Hill and S. H. Lin, *Trans. Faraday Soc.*, **67**, 2833 (1971).
(41) K. R. Butler and M. R. Snow, *J. Chem. Soc. A*, 565 (1971).
(42) J. N. van Niekerk and F. R. L. Schoening, *Acta Crystallogr.*, **5**, 499 (1952).
(43) R. R. Judkins and D. J. Royer, *Inorg. Nucl. Chem. Lett.*, **6**, 305 (1970).
(44) A. D. Liehr, *J. Chem. Phys.*, **68**, 665 (1964).
(45) A. J. McCaffery and S. F. Mason, *Mol. Phys.*, **6**, 359 (1963).
(46) G. Hilmes and F. S. Richardson, *Inorg. Chem.*, **15**, 2582 (1976).
(47) S. F. Mason and R. H. Seal, *Mol. Phys.*, **31**, 755 (1976).
(48) In addition to the work reported here, other examples are given in ref 6, 10, and 55. Also see M. Ito, F. Marumo, and Y. Saito, *Acta Crystallogr., Sect. B*, **27**, 2187 (1971); H. Toftlund and E. Pedersen, *Acta Chem. Scand.*, **26**, 4019 (1972); and S. S. Isied, G. Kuo, and K. N. Raymond, *J. Am. Chem. Soc.*, **98**, 1763 (1976).
(49) F. S. Richardson, *J. Phys. Chem.*, **75**, 692 (1971).
(50) F. S. Richardson, *Inorg. Chem.*, **11**, 2366 (1972).
(51) S. F. Mason and B. J. Norman, *J. Chem. Soc. A*, 307 (1966), and references therein.
(52) W. E. Hatfield, *Inorg. Chem.*, **3**, 605 (1964).
(53) K. Abu-Dari and K. N. Raymond, *Inorg. Chem.*, **16**, 807 (1977).

Contribution from the Laboratoire de Polarographie Organique Associé au CNRS (LA 33), Université de Dijon, 21000 Dijon, France, the Département de Recherche Fondamentale (EOA), Equipe de Recherche Associée au CNRS (ERA 675), Centre d'Etudes Nucléaires de Grenoble, 38041 Grenoble Cedex, France, and the Laboratoire de Cristallographie, Equipe de Recherche Associée au CNRS (ERA 162), Université de Nancy I, 54037 Nancy Cedex, France

Peroxotitanium(IV) Porphyrins. Synthesis, Stereochemistry, and Properties

ROGER GUILARD,*[1a] JEAN-MARC LATOUR,[1b] CLAUDE LECOMTE,[1c] JEAN-CLAUDE MARCHON,*[1b]
JEAN PROTAS,*[1c] and DENIS RIPOLL[1a]

Received July 22, 1977

Reaction of hydrogen peroxide with several oxotitanium(IV) porphyrin complexes $PTi^{IV}O$ under mild conditions affords the corresponding peroxotitanium(IV) complexes $PTi^{IV}(O_2)$. The structures of 2,3,7,8,12,13,17,18-octaethylporphinatoperoxotitanium(IV), $OEPTi(O_2)$, and 2,3,7,8,12,13,17,18-octaethylporphinatooxotitanium(IV), OEPTiO, have been determined from three-dimensional x-ray diffraction data. The peroxo complex crystallizes in the monoclinic space group $P2_1/c$ with four molecules in a unit cell of dimensions $a = 14.603$ (6) Å, $b = 23.266$ (8) Å, $c = 9.793$ (3) Å, and $\beta = 105.0$ (2)°. The structure was solved by direct methods. Least-squares refinement has led to a final value of the conventional R index of 0.064 based on 3415 reflections. The titanium atom is hexacoordinated to the four nitrogen atoms and to the two oxygen atoms. The latter are bonded to the metal in a symmetrical fashion and eclipsed with respect to two nitrogen atoms. The O–O bond length is 1.445 (5) Å, the two Ti–O bond lengths are 1.827 (4) and 1.822 (4) Å, and the average Ti–N bond distance is 2.109 (4) Å. The titanium atom lies at 0.620 (6) Å out of the mean plane of the four nitrogen atoms toward the dioxygen ligand. The oxo complex OEPTiO crystallizes in the monoclinic space group $P2_1/c$ with four molecules in a unit cell of dimensions $a = 14.407$ (6) Å, $b = 23.126$ (8) Å, $c = 9.793$ (3) Å, and $\beta = 104.2$ (2)°. The structure was solved assigning the fractional coordinates found for the $OEPTi(O_2)$ complex to the titanium, nitrogen, and carbon atoms. Least-squares refinement has led to a final value of the conventional R index of 0.067 based on 3570 reflections. The titanium atom is pentacoordinated to the four nitrogen atoms and to the oxygen atom. The Ti–O bond length is 1.613 (5) Å and the average Ti–N bond distance is 2.114 (6) Å. The titanium atom is found to be 0.555 (6) Å out of the plane of the four nitrogen atoms toward the oxygen atom. ^{1}H and ^{13}C dynamic nuclear magnetic resonance studies on $OEPTi(O_2)$ and $TPPTi(O_2)$ (TPP is 5,10,15,20-tetraphenylporphinato) show that these are fluxional molecules. At room temperature and down to about −50 °C, the peroxo ligand undergoes fast exchange between two equivalent sites where the two oxygen atoms eclipse the two equivalent pairs of opposite nitrogen atoms. The barrier to rotation of the peroxo group at the coalescence temperature T_c is 10.8 ± 0.5 kcal mol^{-1} ($T_c = -50$ °C) for $TPPTi(O_2)$ and 9.9 ± 0.5 kcal mol^{-1} ($T_c = -65$ °C) for $OEPTi(O_2)$. Peroxotitanium(IV) porphyrin complexes undergo three successive electron-transfer reactions at a platinum cathode in dichloromethane solution. The first step is bielectronic and irreversible and leads to the corresponding oxotitanium(IV) complex by reductive cleavage of the O–O bond.

Dioxygen complexes of the transition-metal porphyrins are the focus of active current research.[2] These complexes can be considered as synthetic analogues of the hemoproteins which are involved in the transport and activation of molecular oxygen. Much work has been devoted to such model compounds toward a better understanding of the bonding and reactivity of the dioxygen ligand in the biological systems. A major breakthrough was obtained in the isolation and x-ray structure determination of the dioxygen adduct of a ferrous "picket fence" porphyrin.[3] Dioxygen adducts have also been obtained with cobalt(II),[4] chromium(II),[5] and manganese(II) porphyrins.[6] The bonding of O_2 in these complexes is best

Table I. Reaction Conditions and Yields

Compd	Reagent	Reacn solvent	Recrystn solvent	Yield, %	Anal.[a]
$OEPTi(O_2)$	Benzoyl peroxide	1,2,4-Trichlorobenzene	Toluene	30	$(C_{36}H_{44}N_4O_2Ti)$
	H_2O_2	Pyridine		90	C, H, N, Ti
	H_2O_2	CH_2Cl_2		89	
$TPPTi(O_2)$	Benzoyl peroxide	1,2,4-Trichlorobenzene	CH_2Cl_2/MeOH	0	$(C_{44}H_{28}N_4O_2Ti)$
	H_2O_2	Pyridine		90	C, H, N, Ti
	H_2O_2	CH_2Cl_2		91	
$MPOEPTi(O_2)$	Benzoyl peroxide	1,2,4-Trichlorobenzene	Toluene	0	$(C_{42}H_{48}N_4O_2Ti)$
	H_2O_2	Pyridine		63	C, H, N, Ti
	H_2O_2	CH_2Cl_2		62	

[a] This column carries the symbols of elements for which satisfactory analyses were obtained.

described by the superoxide formalism $M^{III}(O_2^{-}\cdot)$ when M is Fe,[7] Co,[4c] or Cr.[5] The peroxide formalism $M^{IV}(O_2^{2-})$ has been suggested for the manganese complex.[6b]

Our interest in titanium porphyrins[8] led us to observe the formation of a complex formulated as $OEPTiO_2$[9] in a number of reactions of the oxotitanium(IV) porphyrin complex $OEPTi^{IV}O$.[8,10] Preliminary results of a single-crystal x-ray diffraction study[10] led to the assignment of the peroxotitanium(IV) formalism to this complex. In this article, we now present a general method which affords peroxo complexes of titanium(IV) porphyrins in high yield from the corresponding oxo complexes and hydrogen peroxide. We also give complete structural results for the $OEPTi(O_2)$ and OEPTiO molecules. Finally, the dynamic stereochemistry and electrochemical behavior of $OEPTi(O_2)$ and $TPPTi(O_2)$[9] are described and discussed.

Experimental Section

Materials. All chemicals and reagents were of reagent grade. Oxo complexes of titanium(IV) porphyrins were prepared as described previously.[8]

Preparation of the Peroxo Complexes of Titanium(IV) Porphyrins. $OEPTi(O_2)$, $TPPTi(O_2)$, and $MPOEPTi(O_2)$[9] were obtained from the corresponding oxo complexes by two methods which are detailed below for $OEPTi(O_2)$.

Method 1 (with Benzoyl Peroxide). OEPTiO (1 mmol, 596 mg) was dissolved in 200 mL of 1,2,4-trichlorobenzene. A solution of benzoyl peroxide (2 mmol, 484 mg) in 100 mL of 1,2,4-trichlorobenzene was added dropwise, and the resulting mixture was kept at 95 °C with stirring for 8 h. The solvent was evaporated under reduced pressure. The oily residue was chromatographed on a silica column. The remaining traces of trichlorobenzene were removed by elution with petroleum ether; then a dichloromethane–petroleum ether (3:2) mixture was used as eluent. The resulting purple solution was evaporated to dryness, and the product was recrystallized from toluene to give a 30% yield of $OEPTi(O_2)$.

Method 2 (with Hydrogen Peroxide). (a) OEPTiO (1 mmol, 596 mg) was dissolved in 100 mL of pyridine at 60 °C, and 15 mL of a pyridine solution of hydrogen peroxide (prepared by tenfold dilution of a commercial H_2O_2 solution approximately 5 M in water) was added dropwise. The mixture was cooled down to room temperature, and the product was precipitated by addition of 100 mL of water. The precipitate was filtered, washed several times with water, and dried. The purple solid was dissolved in dichloromethane–petroleum ether (3:2) and chromatographed on silica as above. Recrystallization from toluene yielded 550 mg of $OEPTi(O_2)$ (90%).

(b) The reaction was also run in dichloromethane. OEPTiO (1 mmol, 596 mg) was dissolved in 100 mL of CH_2Cl_2, and hydrogen peroxide (3 mL of a solution approximately 5 M in water) was added at room temperature. The mixture was stirred for 4 h and then washed with water until no peroxide could be detected (Merckoquant Peroxide Test, reference 10011) in the aqueous phase. After chromatography and recrystallization as above, 545 mg of $OEPTi(O_2)$ was obtained (89%). The reaction conditions, yields, and elemental analyses for the three peroxotitanium(IV) porphyrin complexes are summarized in Table I.

Characterization of the Peroxo Complexes. Characteristic infrared bands and significant fragmentation patterns observed in the mass spectra are listed below.

$OEPTi(O_2)$. IR (CsI pellet): 1025 (w), 1022 (s), 989 (m), 965 (s), 895 (s), 645 (m), 600 (w) cm^{-1}. MS: *A* (mass number) 612 [16.83, $(OEPTiO_2)^{+}\cdot$], 611 [3.09, $(OEPTiO_2 - H)^+$], 596 [100.00, $(OEPTiO_2 - O)^+$].

$TPPTi(O_2)$. IR (CsI pellet): 1000 (s), 895 (s), 635 (m), 595 (w) cm^{-1}. MS: *A* (mass number) 692 [6.97, $(TPPTiO_2)^{+}\cdot$], 690 [5.42, $(TPPTiO_2 - 2H)^+$], 676 [100.00, $(TPPTiO_2 - O)^+$], 599 [12.40, $(TPPTiO_2 - O - C_6H_5)^+$], 598 [9.30, $(TPPTiO_2 - O - C_6H_5 - H)^+$].

$MPOEPTi(O_2)$. IR (CsI pellet): 1010 (s), 975 (m), 955 (s), 855 (s), 630 (m), 585 (w) cm^{-1}. MS: *A* (mass number) 688 [2.37, $(MPOEPTiO_2)^{+}\cdot$], 672 [100.00, $(MPOEPTiO_2 - O)^+$], 671 [16.30, $(MPOEPTiO_2 - O - H)^+$].

Analyses. Elemental analyses were performed by the Service de Microanalyse du CNRS.

Mass Spectrometry. Mass spectra were recorded in the electron-impact mode with a Finnigan 3300 spectrometer and in the field-desorption mode with a JMS Model DISG-2 double-focusing mass spectrometer (MS-FD-01 source). All spectra were obtained by direct inlet in the following conditions. Electron impact: ionizing energy, 70–35 eV; ionizing current, 0.4 mA; source temperature, up to 250 °C. Field desorption: emitter (anode) voltage, +8 kV; cathode voltage, −5 kV; emitter current, 18.5 mA; SEM voltage, 2 kV.

Spectroscopic Studies. ^1H NMR spectra were taken on a JEOL Model C 60 HL spectrometer. Samples (40 mg) were dissolved in 0.4 mL of $CDCl_3$ with tetramethylsilane as internal reference.

Dynamic ^1H and ^{13}C NMR studies were performed with a CAMECA 250 spectrometer. Samples were dissolved in CD_2Cl_2 for the low-temperature measurements and in pyridine-d_5 for the high-temperature measurements. ^1H NMR spectra were obtained with the spectrometer operating at 250 MHz and lock on the tetramethylsilane resonance. Samples containing 15–30 mg of compound in ca. 0.5 mL of solvent were run in 5-mm tubes. ^{13}C NMR spectra were obtained with the spectrometer operating at 62.86 MHz in the ^{13}C pulsed Fourier transform mode with proton noise decoupling and internal deuterium lock. A total of 8192 data points were taken over a 12.5-kHz spectral width using a ca. 10 μs pulse and a ca. 0.6 s acquisition time. Samples containing 20–40 mg of compound in ca. 1.5 mL of solvent were run in 8-mm tubes.

IR spectra were taken either on a Perkin-Elmer 325 or on a Beckman IR 4240 spectrometer. Samples were 1% dispersions in CsI or KBr pellets.

Visible and ultraviolet spectra were recorded on a Beckman Model Acta MIV spectrophotometer. Hydrogen peroxide aliquots were added to a TPPTiO solution in dry pyridine under argon by syringe and the reaction was monitored spectroscopically as follows. The solution was stirred and transferred into a circulation cell (1-mm optical path length) via stainless steel needles and Teflon tubing by depression with a syringe. The reaction vessel and circulation cell were kept at 31.5 ± 0.2 °C with a thermostat.

Electrochemistry. Current–potential curves in dichloromethane solution were recorded with a three-electrode potentiostat (Tacussel PRT 500 LC) driven by a signal generator (Tacussel GSTP). The working electrode was either a rotating platinum electrode or a platinum button (Beckman 39273) for cyclic voltammetric studies. The reference electrode was based on the $Ag/Ag_3I_4^{-}NBu_4^{+}$ system.[11] Tetrabutylammonium hexafluorophosphate was used as background electrolyte. Controlled-potential coulometry was effected with a potentiostat (Tacussel ASA 100) and a coulometer (Tacussel IG3).

Crystallographic Data Collection. Crystals of the peroxo complex $OEPTi(O_2)$ were grown by slow cooling from a solution of the compound in toluene. Weissenberg photographs revealed lattice

Table II. Positional and Thermal[a] Parameters of $OEPTi(O_2)$ (Nonhydrogen Atoms)

	10^4x	10^4y	10^4z	$10^4\beta_{11}$	$10^4\beta_{22}$	$10^4\beta_{33}$	$10^4\beta_{12}$	$10^4\beta_{13}$	$10^4\beta_{23}$
Ti	2513 (1)	9396 (1)	9807 (1)	35 (1)	11 (0)	92 (1)	−2 (0)	0 (0)	5 (0)
O(1)	3350 (2)	9140 (2)	8842 (4)	47 (2)	22 (1)	123 (6)	−1 (1)	7 (3)	4 (2)
O(2)	2399 (3)	9219 (2)	7958 (4)	53 (2)	21 (1)	10 (5)	0 (1)	5 (3)	1 (2)
C(1)	2685 (3)	8257 (2)	11501 (5)	42 (3)	14 (1)	99 (7)	−1 (1)	11 (4)	3 (2)
C(2)	2204 (4)	7709 (2)	11470 (6)	48 (3)	14 (1)	105 (8)	−3 (1)	15 (4)	2 (2)
C(3)	1317 (4)	7780 (2)	10630 (6)	46 (3)	13 (1)	115 (8)	−4 (1)	28 (4)	−1 (2)
C(4)	1239 (4)	8366 (2)	10109 (5)	37 (3)	13 (1)	94 (7)	−1 (1)	12 (4)	2 (2)
C(5)	430 (3)	8616 (2)	9264 (6)	40 (3)	15 (1)	126 (8)	−2 (1)	10 (4)	0 (2)
C(6)	320 (4)	9180 (2)	8787 (6)	35 (3)	15 (1)	121 (8)	−1 (1)	5 (4)	−1 (2)
C(7)	−547 (3)	9437 (2)	7971 (6)	35 (3)	17 (1)	128 (8)	3 (2)	3 (4)	−4 (3)
C(8)	−344 (4)	9999 (2)	7786 (6)	41 (3)	17 (1)	118 (8)	6 (1)	0 (4)	−2 (3)
C(9)	636 (4)	10090 (2)	8484 (6)	44 (3)	14 (1)	116 (8)	4 (1)	0 (4)	1 (2)
C(10)	1129 (4)	10596 (2)	8546 (6)	51 (3)	15 (1)	163 (9)	−3 (2)	−5 (5)	6 (3)
C(11)	2062 (4)	10698 (3)	9240 (7)	62 (4)	13 (1)	170 (10)	−5 (2)	−18 (5)	9 (3)
C(12)	2538 (5)	11244 (2)	9352 (9)	92 (6)	15 (1)	311 (15)	−13 (2)	−51 (8)	46 (4)
C(13)	3433 (5)	11170 (2)	10120 (9)	86 (5)	20 (2)	318 (16)	−25 (2)	−45 (7)	48 (4)
C(14)	3545 (4)	10566 (2)	10503 (6)	55 (4)	17 (1)	153 (9)	−10 (2)	−11 (5)	10 (3)
C(15)	4356 (4)	10315 (2)	11336 (6)	55 (4)	19 (1)	122 (8)	−11 (2)	−6 (4)	15 (3)
C(16)	4441 (4)	9765 (2)	11876 (5)	44 (3)	18 (1)	85 (7)	−8 (2)	−1 (4)	8 (3)
C(17)	5289 (4)	9524 (2)	12806 (6)	41 (3)	22 (1)	100 (8)	−7 (2)	−1 (4)	11 (3)
C(18)	5062 (4)	8973 (2)	13077 (6)	42 (3)	21 (1)	144 (10)	−3 (2)	−6 (5)	18 (3)
C(19)	4094 (4)	8885 (2)	12338 (6)	43 (3)	17 (1)	113 (8)	−1 (2)	−3 (4)	14 (3)
C(20)	3597 (4)	8372 (2)	12281 (6)	47 (3)	16 (1)	127 (9)	−3 (2)	2 (4)	8 (3)
N(21)	2078 (3)	8652 (2)	10648 (4)	34 (2)	11 (1)	102 (6)	−1 (1)	9 (3)	5 (2)
N(22)	1040 (3)	9581 (2)	9122 (4)	34 (2)	13 (1)	109 (6)	0 (1)	1 (3)	−1 (2)
N(23)	2696 (3)	10289 (2)	9965 (5)	49 (3)	11 (1)	126 (7)	−5 (1)	−10 (3)	4 (2)
N(24)	3711 (3)	9369 (2)	11597 (4)	38 (2)	19 (1)	99 (6)	−5 (1)	−2 (3)	5 (2)
C(25)	2661 (4)	7173 (2)	12192 (6)	62 (4)	13 (1)	145 (9)	1 (2)	24 (5)	13 (3)
C(26)	3253 (5)	6873 (3)	11320 (8)	83 (5)	21 (1)	241 (13)	13 (2)	37 (7)	19 (4)
C(27)	548 (4)	7333 (2)	10232 (6)	54 (4)	15 (1)	144 (9)	−8 (2)	23 (4)	2 (3)
C(28)	531 (6)	7056 (3)	8815 (8)	102 (6)	26 (2)	187 (12)	−14 (3)	20 (7)	−19 (4)
C(29)	−1458 (4)	9116 (3)	7379 (8)	31 (3)	24 (2)	220 (12)	1 (2)	10 (5)	5 (4)
C(30)	−1487 (5)	8798 (3)	5997 (8)	72 (5)	30 (2)	201 (12)	−8 (2)	0 (6)	−25 (4)
C(31)	−1009 (4)	10453 (3)	6973 (7)	51 (4)	19 (1)	161 (10)	9 (2)	−3 (5)	4 (3)
C(32)	−966 (5)	10508 (3)	5442 (7)	98 (6)	26 (1)	145 (10)	15 (2)	3 (6)	13 (3)
C(33)	1898 (7)	11905 (4)	9065 (10)	103 (7)	48 (3)	239 (17)	−30 (4)	−25 (9)	32 (6)
C(34)	2154 (7)	11925 (6)	7809 (14)	106 (8)	92 (5)	382 (26)	−28 (5)	111 (12)	−75 (10)
C(35)	4204 (8)	11708 (5)	10901 (13)	129 (9)	42 (3)	374 (24)	17 (4)	13 (11)	68 (7)
C(36)	4658 (7)	11695 (6)	9879 (12)	108 (8)	85 (5)	225 (18)	20 (5)	53 (10)	−6 (7)
C(37)	6228 (4)	9827 (3)	13329 (7)	51 (4)	26 (2)	158 (10)	−15 (2)	2 (5)	23 (3)
C(38)	6275 (5)	10179 (4)	14629 (9)	74 (5)	38 (2)	222 (13)	−20 (3)	8 (6)	−13 (5)
C(39)	5730 (4)	8510 (3)	13918 (8)	61 (4)	31 (2)	168 (11)	−4 (2)	−3 (5)	24 (4)
C(40)	5696 (6)	8506 (4)	15389 (9)	97 (6)	45 (3)	230 (15)	11 (3)	34 (8)	46 (5)

[a] The form of the anisotropic thermal ellipsoid is $\exp[-(\beta_{11}h^2 + \beta_{22}k^2 + \beta_{33}l^2 + \beta_{12}hk + \beta_{13}hl + \beta_{23}kl)]$.

symmetry $2/m$ and systematic absences $h0l$ ($l = 2n + 1$) and $0k0$ ($k = 2n + 1$) defining uniquely the monoclinic space group $P2_1/c$. Preliminary cell dimensions, measured from Weissenberg photographs and subsequently adjusted by the least-squares procedure applied to the setting angles of 31 reflections measured on a three-circle CAD-3 Enraf–Nonius diffractometer using Cu Kα radiation, are a = 14.603 (6) Å, b = 23.266 (8) Å, c = 9.793 (3) Å, β = 105.0 (2)°, and V = 3213 Å^3. The calculated specific gravity is 1.26 g cm^{-3} based on four molecules per unit cell. The crystal used for the intensity measurements was a parallelepiped of approximate dimensions 0.2 × 0.3 × 0.5 mm^3 ($0.5 < \mu R < 1.3$). It was elongated along the [001] crystallographic axis. Intensity measurements were made by a (θ, 2θ) step-scan procedure, with the nickel-filtered Cu Kα (λ 1.540 51 Å) radiation on a three-circle CAD-3 Enraf–Nonius diffractometer at room temperature. During the intensity measurements, one reflection was used for periodic checking (every 50 reflections) on the alignment and possible deterioration of the crystal; no deviations greater than statistical were observed. A total of 4706 reflections were measured in one quarter of the diffraction sphere with $4° < \theta < 57°$, and 3415 reflections with $\sigma(I)/I < 0.25$ were used to solve and to refine the structure. These reflections were corrected for Lorentz and polarization effects. Absorption corrections were not applied.

In the case of the oxo complex, the study was first performed on an orthorhombic form of OEPTiO.[12] Owing to the poor quality of this first modification, the compound was recrystallized from the same solvent as $OEPTi(O_2)$ (toluene). The crystals were isotypic with $OEPTi(O_2)$: monoclinic, $P2_1/c$, a = 14.407 (6) Å, b = 23.126 (8) Å, c = 9.793 (3) Å, β = 104.2 (2)°, V = 3164 Å^3, d_{calcd} = 1.27 g cm^{-3}, Z = 4 formula units per unit cell. The crystal used for intensity measurements had approximate dimensions 0.3 × 0.4 × 0.6 mm^3 ($0.7 < \mu R < 1.5$). It was also elongated along the c axis. The intensity measurement techniques were similar to those described for $OEPTi(O_2)$: 4669 reflections were recorded inside the range $4° < \theta < 57°$; 3570 reflections with $\sigma(I)/I < 0.25$ were used to refine the structure.

Solution and Refinement of the Crystal Structures. The crystal structure of $OEPTi(O_2)$ was solved by direct methods using the MULTAN[13] computer program. Fourier syntheses were applied to the best set of phases and gave the approximate positions of the titanium atom, the two oxygen atoms, and the four pyrrole groups. The R index was 0.242. Difference Fourier syntheses showed clearly the missing atoms. A least-squares procedure using the diagonal-matrix method was first applied[10] and then followed by least-squares refinement using full-matrix methods.[14] The function minimized was $\sum w(F_o - F_c)^2$, where $w = 1/\sigma^2(F_0)$. This procedure allowed us to localize 33 of the 44 hydrogen atoms in Fourier difference syntheses. These atoms were included in the refinement process; a correction for anomalous dispersion was made for the titanium atom (Δf = 0.2, $\Delta f'$ = 1.9) and the final R index was 0.064. Final positional and anisotropic thermal parameters for the nonhydrogen atoms are given in Table II; positional parameters of hydrogen atoms are given in Table III.[15]

The crystal structure of OEPTiO was solved assigning the fractional coordinates (x, y, z) found for the $OEPTi(O_2)$ complex to the titanium, nitrogen, and carbon atoms; the R index was 0.237. Difference Fourier syntheses then clearly showed the missing oxygen atom. The refinement of all nonhydrogen atoms using the same least-squares procedure as above for $OEPTi(O_2)$ led to an R index of 0.098. Difference Fourier syntheses then showed most of the hydrogen atoms;

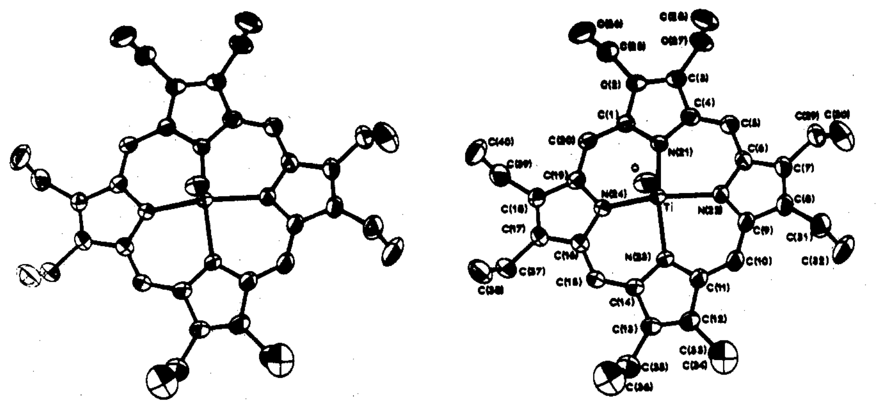

Figure 1. Stereoscopic view of the OEPTiO molecule. The vibrational ellipsoids are drawn at the 50% probability level. All hydrogen atoms have been omitted. The numbering scheme is indicated.

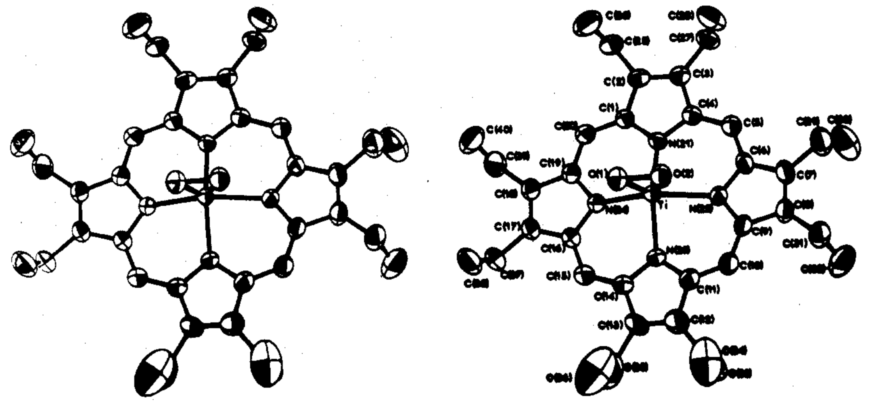

Figure 2. Stereoscopic view of the $OEPTi(O_2)$ molecule. The vibrational ellipsoids are drawn at the 50% probability level. All hydrogen atoms have been omitted. The numbering scheme is indicated.

these were included in the refinement process. A correction for anomalous dispersion of the titanium atom was made. The final R index was 0.067. Final positional and thermal parameters for the nonhydrogen atoms are given in Table IV. Positional parameters of the hydrogen atoms are given in Table V.[15] A list of calculated and observed structure factors for the two crystal structures is available.[15]

Results

Syntheses and Structure Assignment. Reaction of hydrogen peroxide under mild conditions (20–60 °C) on oxotitanium(IV) porphyrin complexes PTiO[9] affords compounds corresponding to a formula $PTiO_2H_x$ (x = 0–2). Analytically pure samples are obtained by chromatography on silica. The yields are high (70–90%) and do not seem to depend on the nature of the starting complex. The compound obtained from OEPTiO can also be made by reaction with benzoyl peroxide. Heating to 95 °C is then necessary, and the yield is lower (Table I).

Elemental analyses, in conjunction with valency considerations, lead to a formulation as either $PTi(O_2)$ or $PTi(OH)_2$. Mass spectrometric results are in favor of the $PTi(O_2)$ formula. Isotopic distribution patterns relative to the highest observed m/e value correspond to $M^{+\cdot} = PTiO_2^{+\cdot}$; no pattern is observed for M + 2, which tends to exclude the $PTi(OH)_2$ formula. In every case, the base peak is that of the $[PTiO_2 - O]^{+\cdot}$ ion. Characteristic fragmentations of substituted porphyrins are observed at lower m/e values, particularly $[P - CH_2 - R]^{+\cdot} \rightarrow [P - CH_2]^+ + R\cdot$ in the case of $OEPTi(O_2)$.[9,16]

The formulation of these molecules as $PTi(O_2)$, as well as the use of peroxide compounds for their preparation, leads to their formal description as peroxotitanium(IV) complexes. Infrared spectra corroborate this description. $OEPTi(O_2)$ exhibits three absorption bands at 895, 645, and 600 cm^{-1} which are absent from the OEPTiO spectrum. These characteristic bands are found at 895, 635, and 595 cm^{-1} for $TPPTi(O_2)$ and at 885, 630, and 585 cm^{-1} for $MPOEPTi(O_2)$. The presence of these three vibrational modes for the $Ti(O_2)$ group suggests an isosceles triangular geometry.[17a] By analogy with other peroxotitanium(IV) complexes, the band near 900 cm^{-1} is assigned to O–O stretching and the other two bands to symmetric and asymmetric M–O stretch.[17]

Crystal Structure Analysis. The crystal structure of $OEPTi(O_2)$ was determined to corroborate the studies by mass spectrometry and IR spectroscopy. Furthermore, the crystal structure of OEPTiO was refined to determine the modifications resulting from the presence of an oxide ligand instead of a peroxide. Figures 1 and 2 show stereoscopic views of the molecules OEPTiO and $OEPTi(O_2)$ and the numbering scheme used in this paper. Tables VI–IX give the values and the standard deviations of the bond distances and angles in the two titanium complexes.

In OEPTiO, the titanium atom is pentacoordinated by the four nitrogen atoms and the oxygen atom. The coordination polyhedron is a pyramid with a square basis whose symmetry is very close to C_{4v}. The titanium–oxygen distance is 1.613 (5) Å and the Ti–N mean distance 2.114 (6) ± 0.006 Å. The titanium atom lies at 0.555 (6) Å from the plane defined by the four nitrogen atoms and at 0.603 (6) Å from the mean plane of the porphine skeleton; the radius of the central hole is Ct–N = 2.040 (5) Å. Finally, the Ti, O, N(21), and N(23) atoms on one hand and the Ti, O, N(22), and N(24) atoms on the other are coplanar, and these resulting planes are perpendicular to the mean plane of the porphine skeleton (Table X).[15]

In the $OEPTi(O_2)$ complex, the degree of symmetry of the coordination polyhedron of the titanium atom is reduced to C_{2v}. The titanium is hexacoordinated by the four nitrogen atoms and the two oxygen atoms symmetrically bonded on the

Table IV. Positional and Thermal[a] Parameters of OEPTiO (Nonhydrogen Atoms)

	10^4x	10^4y	10^4z	$10^4\beta_{11}$	$10^4\beta_{22}$	$10^4\beta_{33}$	$10^4\beta_{12}$	$10^4\beta_{13}$	$10^4\beta_{23}$
Ti	2495 (1)	9416 (0)	9879 (1)	35 (1)	9 (0)	83 (1)	−2 (0)	3 (1)	2 (0)
O	2894 (3)	9213 (2)	8553 (4)	69 (3)	16 (1)	114 (6)	−5 (1)	33 (4)	−1 (2)
C(1)	2640 (4)	8252 (2)	11527 (6)	45 (4)	12 (1)	89 (8)	−1 (2)	16 (5)	4 (3)
C(2)	2146 (4)	7702 (2)	11497 (6)	46 (4)	11 (1)	93 (9)	−3 (2)	20 (5)	5 (2)
C(3)	1261 (4)	7769 (2)	10636 (6)	42 (4)	10 (1)	92 (8)	−3 (2)	24 (4)	1 (2)
C(4)	1201 (4)	8360 (2)	10120 (6)	36 (3)	11 (1)	89 (8)	−1 (2)	14 (4)	−1 (2)
C(5)	399 (4)	8611 (2)	9239 (6)	38 (3)	11 (1)	109 (8)	−3 (2)	9 (4)	−2 (2)
C(6)	302 (4)	9183 (2)	8750 (6)	36 (3)	13 (1)	106 (8)	−2 (2)	6 (4)	−4 (2)
C(7)	−566 (4)	9436 (3)	7906 (6)	33 (3)	14 (1)	110 (8)	1 (2)	1 (4)	−3 (3)
C(8)	−370 (4)	10003 (3)	7741 (7)	38 (4)	15 (1)	108 (9)	6 (2)	−3 (5)	−1 (3)
C(9)	616 (4)	10100 (3)	8463 (6)	46 (4)	13 (1)	99 (8)	3 (2)	−1 (5)	1 (3)
C(10)	1097 (5)	10622 (3)	8582 (7)	56 (4)	11 (1)	126 (9)	−1 (2)	−15 (5)	6 (3)
C(11)	2033 (5)	10737 (3)	9311 (7)	64 (5)	12 (1)	120 (9)	−4 (2)	−15 (5)	5 (3)
C(12)	2486 (6)	11304 (3)	9518 (8)	77 (6)	12 (1)	185 (13)	−9 (2)	−35 (7)	16 (3)
C(13)	3391 (6)	11229 (3)	10294 (8)	74 (6)	15 (2)	170 (12)	−16 (2)	−27 (7)	15 (3)
C(14)	3528 (5)	10606 (3)	10602 (7)	59 (4)	15 (1)	115 (9)	−10 (2)	−17 (5)	9 (3)
C(15)	4346 (5)	10346 (3)	11402 (7)	53 (4)	18 (1)	121 (9)	−13 (2)	−16 (5)	12 (3)
C(16)	4442 (4)	9778 (3)	11882 (6)	42 (4)	16 (1)	91 (8)	−9 (2)	−4 (5)	5 (3)
C(17)	5288 (4)	9530 (3)	12778 (7)	37 (4)	20 (2)	111 (9)	−6 (2)	−6 (7)	6 (5)
C(18)	5061 (4)	8971 (3)	13055 (7)	36 (4)	18 (2)	114 (9)	−2 (2)	−4 (5)	7 (3)
C(19)	4072 (4)	8882 (3)	12327 (6)	40 (4)	15 (1)	96 (8)	0 (2)	2 (4)	9 (3)
C(20)	3570 (4)	8363 (3)	12306 (6)	39 (4)	14 (1)	109 (9)	−2 (2)	9 (5)	4 (3)
N(21)	2047 (3)	8642 (2)	10672 (5)	33 (3)	10 (1)	88 (6)	0 (1)	10 (3)	4 (2)
N(22)	1019 (3)	9587 (2)	9080 (5)	35 (3)	11 (1)	102 (6)	0 (1)	−2 (3)	2 (2)
N(23)	2683 (3)	10325 (2)	10011 (5)	48 (3)	10 (1)	109 (7)	−5 (1)	−9 (3)	3 (2)
N(24)	3702 (3)	9378 (2)	11602 (5)	36 (3)	13 (1)	94 (7)	−4 (1)	−1 (3)	6 (2)
C(25)	2590 (5)	7165 (3)	12249 (7)	59 (4)	12 (1)	146 (10)	2 (2)	25 (6)	17 (3)
C(26)	3221 (6)	6849 (3)	11437 (9)	75 (6)	16 (2)	212 (13)	11 (2)	33 (7)	12 (4)
C(27)	488 (5)	7318 (3)	10232 (7)	48 (4)	15 (1)	119 (9)	−7 (2)	19 (5)	1 (3)
C(28)	470 (6)	7044 (3)	8810 (8)	85 (6)	17 (2)	167 (12)	−9 (2)	22 (7)	−13 (4)
C(29)	−1494 (5)	9113 (3)	7313 (8)	37 (4)	20 (2)	165 (11)	1 (2)	6 (5)	6 (3)
C(30)	−1481 (5)	8782 (3)	5949 (8)	54 (5)	28 (2)	163 (12)	−7 (3)	−1 (6)	−27 (4)
C(31)	−1036 (5)	10458 (3)	6923 (8)	46 (4)	16 (2)	155 (11)	6 (2)	−1 (5)	2 (3)
C(32)	−988 (6)	10510 (3)	5385 (8)	77 (6)	23 (2)	151 (11)	10 (3)	11 (6)	13 (4)
C(33)	1951 (6)	11889 (3)	9072 (9)	80 (6)	21 (2)	172 (13)	−6 (3)	1 (6)	15 (4)
C(34)	2154 (7)	12066 (5)	7656 (10)	98 (8)	48 (3)	218 (16)	3 (4)	65 (9)	16 (6)
C(35)	4140 (7)	11706 (4)	10896 (9)	93 (7)	22 (2)	177 (13)	−4 (3)	2 (8)	9 (4)
C(36)	4818 (7)	11757 (5)	9995 (10)	83 (7)	47 (3)	173 (13)	−3 (4)	42 (8)	5 (5)
C(37)	6255 (5)	9830 (3)	13322 (9)	49 (4)	24 (2)	161 (11)	−14 (2)	−2 (6)	17 (4)
C(38)	6250 (6)	10180 (4)	14648 (10)	74 (6)	33 (2)	199 (14)	−23 (3)	−22 (7)	−14 (5)
C(39)	5726 (5)	8515 (3)	13897 (8)	44 (4)	22 (2)	143 (11)	1 (2)	−6 (5)	11 (3)
C(40)	5701 (6)	8519 (4)	15422 (9)	78 (6)	38 (3)	153 (12)	12 (3)	22 (7)	32 (5)

[a] The form of the anisotropic thermal ellipsoid is $\exp[-(\beta_{11}h^2 + \beta_{22}k^2 + \beta_{33}l^2 + \beta_{12}hk + \beta_{13}hl + \beta_{23}kl)]$.

titanium atom. The O–O distance is 1.445 (5) Å and the Ti–O mean distance is 1.825 (4) ± 0.003 Å. The peroxide group eclipses almost perfectly the N(22) and N(24) nitrogen atoms. Indeed, these atoms lie respectively at 0.026 and 0.001 Å from the plane defined by the Ti, O(1), and O(2) atoms. Contrary to OEPTiO, the Ti-N bond lengths do not seem to be equivalent: the mean value of the Ti–N(22) and Ti–N(24) distances is 2.128 (4) ± 0.005 Å and the mean value of the Ti–N(21) and the Ti–N(23) distances is 2.090 (4) ± 0.004 Å. The titanium atom lies at 0.620 (6) Å from the plane of the four nitrogen atoms and at 0.657 (6) Å from the mean plane of the macrocycle (Table XI).[15]

The thermal parameters of the ethyl groups of OEPTiO and particularly those of OEPTi(O_2) are very large so that the values of the ethyl–methyl bond distances and angles are known with very low accuracy. The methyl groups of six ethyl groups are on the same side as the axial ligand with regard to the macrocycle plane. This orientation is at the origin of intermolecular contacts with the oxide ligand (Table XII)[15] or with the peroxide ligand (Table XIII).[15]

Dynamic Nuclear Magnetic Resonance Spectroscopy. ^1H NMR characteristics of the PTi(O_2) complexes at ambient temperatures are listed in Table XIV. The observed sharpness of the resonance lines is consistent with the diamagnetism of the complexes as measured in the solid state. For the sake of comparison, the ^1H NMR characteristics of the starting PTiO complexes are also reported in Table XIV. A slight shielding of all protons is observed upon substitution by the peroxo ligand.

For TPPTi(O_2) and MPOEPTi(O_2), the resonance lines corresponding to the ortho phenyl protons are broad at 60 MHz and split in a doublet at higher resolution. This reflects the already well-documented phenomenon of restricted rotation of phenyl rings which has been studied in detail for various PTiO complexes.[8,18] The barrier to rotation was determined by an approximate treatment of NMR data[19] for TPPTi(O_2) in deuterated pyridine solution. Its value ($\Delta G_c^\ddagger = 15.8 \pm 0.5$ kcal mol^{-1} at $T_c = 40$ °C) is very close to those obtained earlier for analogous complexes.[8,18]

The ambient-temperature ^1H NMR spectrum of TPPTi(O_2) exhibits a single peak for the pyrrole protons. Upon cooling, this peak broadens and splits in a doublet below −50 °C (Figure 3). The observed dynamic equilibrium seems to be related to the presence of the peroxo group and to the existence of two possible sites for this ligand in the TPPTi(O_2) molecule (vide infra). The coalescence temperature is the same, within experimental error, for a saturated solution prepared at 25 °C and after about tenfold dilution. This suggests that the observed exchange takes place by an intramolecular mechanism. An approximate treatment of the data[19] gives an activation energy $\Delta G_c^\ddagger = 10.8 \pm 0.5$ kcal mol^{-1} for the process at the coalescence temperature $T_c = -50$ °C.

The ambient-temperature ^1H NMR spectrum of OEPTi(O_2) exhibits a complex multiplet for the methylene protons,

Table VI. Interatomic Distances (Å) in OEPTi(O_2)[a]

O(1)–O(2)	1.445 (5)		
Ti–O(1)	1.827 (4)	Ti–O(2)	1.822 (4)
Ti–N(21)	2.086 (4)	Ti–N(23)	2.094 (4)
Ti–N(22)	2.123 (4)	Ti–N(24)	2.133 (4)
Ti–C(5)	3.463 (5)	Ti–C(15)	3.458 (6)
Ti–C(10)	3.479 (5)	Ti–C(20)	3.475 (6)
N(21)–C(1)	1.393 (6)	N(22)–C(6)	1.379 (6)
C(1)–C(2)	1.452 (7)	C(6)–C(7)	1.440 (7)
C(2)–C(3)	1.352 (7)	C(7)–C(8)	1.362 (8)
C(3)–C(4)	1.451 (7)	C(8)–C(9)	1.434 (7)
C(4)–N(21)	1.374 (6)	C(9)–N(22)	1.396 (6)
C(4)–C(5)	1.383 (6)	C(9)–C(10)	1.373 (8)
C(5)–C(6)	1.389 (7)	C(1)–C(20)	1.379 (7)
N(23)–C(11)	1.388 (7)	N(24)–C(16)	1.381 (7)
C(11)–C(12)	1.438 (9)	C(16)–C(17)	1.447 (7)
C(12)–C(13)	1.339 (10)	C(17)–C(18)	1.366 (8)
C(13)–C(14)	1.452 (9)	C(18)–C(19)	1.426 (7)
C(14)–N(23)	1.375 (7)	C(19)–N(24)	1.377 (7)
C(14)–C(15)	1.381 (7)	C(19)–C(20)	1.392 (8)
C(11)–C(10)	1.377 (8)	C(15)–C(16)	1.377 (8)
C(2)–C(25)	1.502 (7)	C(12)–C(33)	1.78 (2)
C(25)–C(26)	1.531 (10)	C(33)–C(34)	1.38 (2)
C(3)–C(27)	1.505 (7)	C(13)–C(35)	1.72 (2)
C(27)–C(28)	1.524 (10)	C(35)–C(36)	1.34 (2)
C(7)–C(29)	1.506 (7)	C(17)–C(37)	1.508 (8)
C(29)–C(30)	1.533 (11)	C(37)–C(38)	1.500 (11)
C(8)–C(31)	1.515 (7)	C(18)–C(39)	1.542 (9)
C(31)–C(32)	1.522 (10)	C(39)–C(40)	1.454 (12)
O(1)–N(21)	3.092 (5)	O(2)–N(21)	3.089 (5)
O(1)–N(22)	3.601 (6)	O(2)–N(22)	2.667 (5)
O(1)–N(23)	3.132 (5)	O(2)–N(23)	3.141 (6)
O(1)–N(24)	2.664 (5)	O(2)–N(24)	3.599 (5)
N(21)–N(22)	2.833 (6)	N(21)–N(23)	4.010 (6)
N(22)–N(23)	2.865 (6)	N(22)–N(24)	4.053 (6)
N(23)–N(24)	2.847 (6)	N(24)–N(21)	2.860 (6)

[a] The numbers in parentheses are the estimated standard deviations.

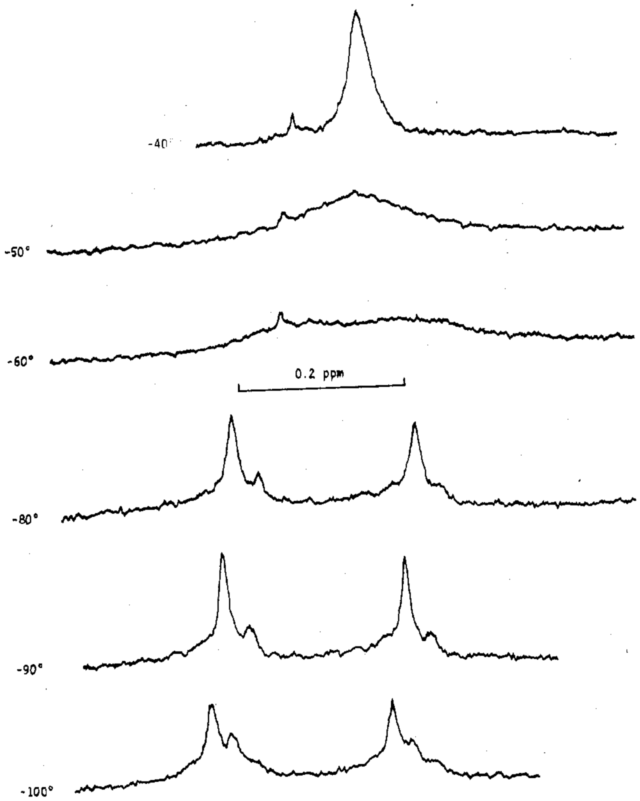

Figure 3. Temperature dependence of the pyrrole proton resonance lines of TPPTi(O_2) in CD_2Cl_2. The weak peaks correspond to an unidentified impurity.

Table VII. Bond Angles (deg) in OEPTi(O_2)[a]

O(1)–Ti–N(21)	104.2 (2)	O(2)–Ti–N(21)	104.2 (2)
O(1)–Ti–N(22)	131.3 (2)	O(2)–Ti–N(22)	84.7 (2)
O(1)–Ti–N(23)	105.8 (2)	O(2)–Ti–N(23)	106.0 (2)
O(1)–Ti–N(24)	84.2 (2)	O(2)–Ti–N(24)	130.8 (2)
N(21)–Ti–N(22)	84.6 (2)	N(23)–Ti–N(24)	84.7 (2)
N(22)–Ti–N(23)	85.6 (2)	N(21)–Ti–N(24)	85.3 (2)
N(21)–Ti–N(23)	147.2 (2)	N(22)–Ti–N(24)	144.5 (2)
C(1)–N(21)–C(4)	106.1 (4)	C(6)–N(22)–C(9)	105.0 (4)
C(1)–C(2)–C(3)	106.7 (5)	N(22)–C(6)–C(7)	111.0 (4)
C(2)–C(3)–C(4)	107.7 (5)	C(6)–C(7)–C(8)	106.4 (5)
C(3)–C(4)–N(21)	109.8 (4)	C(7)–C(8)–C(9)	107.6 (5)
N(21)–C(1)–C(2)	109.8 (4)	C(8)–C(9)–N(22)	110.0 (5)
N(23)–C(11)–C(12)	108.8 (5)	C(16)–N(24)–C(19)	104.7 (4)
C(11)–N(23)–C(14)	106.8 (5)	N(24)–C(16)–C(17)	110.9 (4)
C(11)–C(12)–C(13)	108.1 (6)	C(16)–C(17)–C(18)	105.9 (5)
C(12)–C(13)–C(14)	107.3 (6)	C(17)–C(18)–C(19)	107.2 (5)
C(13)–C(14)–N(23)	108.9 (5)	C(18)–C(19)–N(24)	111.3 (5)
C(4)–C(5)–C(6)	127.2 (5)	C(1)–C(20)–C(19)	127.4 (5)
C(9)–C(10)–C(11)	127.6 (5)	C(14)–C(15)–C(16)	126.7 (5)
C(1)–C(2)–C(25)	124.5 (5)	C(11)–C(12)–C(33)	121.7 (6)
C(3)–C(2)–C(25)	128.7 (5)	C(13)–C(12)–C(33)	130.0 (10)
C(2)–C(25)–C(26)	111.2 (5)	C(12)–C(33)–C(34)	85.2 (10)
C(2)–C(3)–C(27)	127.3 (5)	C(12)–C(13)–C(35)	125.8 (7)
C(4)–C(3)–C(27)	124.9 (5)	C(14)–C(13)–C(35)	124.8 (7)
C(3)–C(27)–C(28)	111.2 (5)	C(13)–C(35)–C(36)	92.5 (10)
C(2)–C(1)–C(20)	125.0 (5)	C(12)–C(11)–C(10)	126.0 (6)
N(21)–C(1)–C(20)	125.3 (5)	N(23)–C(11)–C(10)	125.2 (5)
N(21)–C(4)–C(5)	124.5 (5)	N(23)–C(14)–C(15)	125.3 (5)
C(3)–C(4)–C(5)	125.7 (5)	C(13)–C(14)–C(15)	125.7 (6)
C(5)–C(6)–C(7)	126.0 (5)	C(15)–C(16)–C(17)	125.4 (5)
C(5)–C(6)–N(22)	123.0 (5)	C(15)–C(16)–N(24)	123.7 (5)
C(6)–C(7)–C(29)	124.7 (5)	C(16)–C(17)–C(37)	126.0 (5)
C(7)–C(29)–C(30)	113.5 (5)	C(17)–C(37)–C(38)	112.4 (5)
C(8)–C(7)–C(29)	128.7 (5)	C(18)–C(17)–C(37)	128.1 (5)
C(7)–C(8)–C(31)	127.4 (5)	C(17)–C(18)–C(39)	127.4 (5)
C(8)–C(31)–C(32)	113.0 (5)	C(18)–C(39)–C(40)	110.7 (6)
C(9)–C(8)–C(31)	125.0 (5)	C(19)–C(18)–C(39)	125.2 (5)
C(10)–C(9)–C(8)	126.4 (5)	C(20)–C(19)–C(18)	125.6 (5)
C(10)–C(9)–N(22)	123.5 (5)	C(20)–C(19)–N(24)	122.9 (5)
Ti–O(1)–O(2)	66.5 (2)	O(1)–O(2)–Ti	66.9 (2)
O(1)–Ti–O(2)	46.7 (2)		

[a] The numbers in parentheses are the estimated standard deviations.

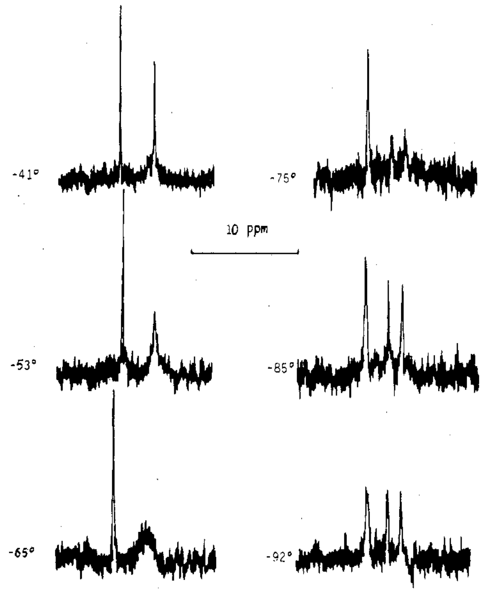

Figure 4. Temperature dependence of the α and β pyrrole carbon resonance lines of OEPTi(O_2) in CD_2Cl_2. The C_β lines are those at higher field (right).

reflecting their anisochronous behavior related to asymmetrical axial ligation.[20] Upon cooling, this signal broadens and loses its structure; no splitting is observed down to the freezing point of the solution (about −100 °C). In contrast, ^{13}C NMR spectra of OEPTi(O_2) recorded in the same conditions show a splitting of the β-carbon peak below −65 °C (Figure 4). The

Table VIII. Interatomic Distances (Å) in OEPTiO[a]

Ti-O	1.613 (5)		
Ti-N(21)	2.112 (5)	Ti-N(23)	2.120 (5)
Ti-N(22)	2.116 (5)	Ti-N(24)	2.109 (4)
Ti-C(5)	3.470 (6)	Ti-C(15)	3.467 (7)
Ti-C(10)	3.492 (7)	Ti-C(20)	3.487 (6)
N(21)-C(1)	1.376 (7)	N(22)-C(6)	1.370 (7)
C(1)-C(2)	1.455 (8)	C(6)-C(7)	1.444 (8)
C(2)-C(3)	1.354 (8)	C(7)-C(8)	1.358 (9)
C(3)-C(4)	1.452 (8)	C(8)-C(9)	1.441 (8)
C(4)-N(21)	1.370 (7)	C(9)-N(22)	1.392 (7)
C(4)-C(5)	1.389 (7)	C(5)-C(6)	1.400 (8)
C(1)-C(20)	1.393 (8)	C(9)-C(10)	1.382 (9)
N(23)-C(11)	1.392 (8)	N(24)-C(16)	1.387 (8)
C(11)-C(12)	1.457 (9)	C(16)-C(17)	1.434 (8)
C(12)-C(13)	1.350 (10)	C(17)-C(18)	1.376 (9)
C(13)-C(14)	1.475 (9)	C(18)-C(19)	1.443 (8)
C(14)-N(23)	1.375 (8)	C(19)-N(24)	1.383 (7)
C(14)-C(15)	1.383 (9)	C(19)-C(20)	1.400 (9)
C(11)-C(10)	1.387 (9)	C(15)-C(16)	1.391 (9)
C(2)-C(25)	1.505 (8)	C(12)-C(33)	1.565 (10)
C(25)-C(26)	1.531 (11)	C(33)-C(34)	1.541 (14)
C(3)-C(27)	1.506 (8)	C(13)-C(35)	1.554 (11)
C(27)-C(28)	1.525 (10)	C(35)-C(36)	1.473 (15)
C(7)-C(29)	1.516 (8)	C(17)-C(37)	1.531 (9)
C(29)-C(30)	1.544 (11)	C(37)-C(38)	1.531 (12)
C(8)-C(31)	1.515 (8)	C(18)-C(39)	1.524 (9)
C(31)-C(32)	1.530 (11)	C(39)-C(40)	1.504 (12)
O-N(21)	2.962 (6)	O-N(22)	2.999 (6)
O-N(23)	2.993 (7)	O-N(24)	2.952 (6)
N(21)-N(22)	2.874 (7)	N(24)-N(21)	2.890 (7)
N(22)-N(23)	2.903 (7)	N(21)-N(23)	4.085 (7)
N(23)-N(24)	2.874 (7)	N(22)-N(24)	4.076 (7)

[a] The numbers in parentheses are the estimated standard deviations.

Table IX. Bond Angles (deg) in OEPTiO[a]

O-Ti-N(21)	104.5 (2)	O-Ti-N(23)	105.8 (2)
O-Ti-N(22)	106.3 (2)	O-Ti-N(24)	104.2 (2)
N(21)-Ti-N(22)	85.6 (2)	N(23)-Ti-N(24)	85.6 (2)
N(22)-Ti-N(23)	86.5 (2)	N(24)-Ti-N(21)	86.4 (2)
N(21)-Ti-N(23)	149.7 (2)	N(22)-Ti-N(24)	149.5 (2)
C(1)-N(21)-C(4)	106.8 (5)	C(6)-N(22)-C(9)	105.6 (5)
C(1)-C(2)-C(3)	107.1 (5)	N(22)-C(6)-C(7)	110.9 (5)
C(2)-C(3)-C(4)	107.0 (5)	C(6)-C(7)-C(8)	106.4 (5)
C(3)-C(4)-N(21)	109.8 (5)	C(7)-C(8)-C(9)	107.6 (5)
N(21)-C(1)-C(2)	109.4 (5)	C(8)-C(9)-N(22)	109.6 (5)
C(11)-N(23)-C(14)	107.8 (5)	C(16)-N(24)-C(19)	105.6 (5)
N(23)-C(11)-C(12)	108.7 (6)	N(24)-C(16)-C(17)	110.5 (5)
C(11)-C(12)-C(13)	107.5 (6)	C(16)-C(17)-C(18)	106.8 (6)
C(12)-C(13)-C(14)	107.6 (6)	C(17)-C(18)-C(19)	106.8 (5)
C(13)-C(14)-N(23)	108.3 (6)	C(18)-C(19)-N(24)	110.2 (5)
C(4)-C(5)-C(6)	127.2 (5)	C(1)-C(20)-C(19)	126.2 (6)
C(9)-C(10)-C(11)	127.8 (6)	C(14)-C(15)-C(16)	127.0 (6)
C(1)-C(2)-C(25)	124.4 (5)	C(11)-C(12)-C(33)	124.5 (6)
C(3)-C(2)-C(25)	128.5 (6)	C(13)-C(12)-C(33)	127.8 (6)
C(2)-C(25)-C(26)	112.0 (6)	C(12)-C(33)-C(34)	106.9 (7)
C(2)-C(3)-C(27)	127.4 (5)	C(12)-C(13)-C(35)	127.5 (7)
C(4)-C(3)-C(27)	125.6 (5)	C(14)-C(13)-C(35)	124.7 (7)
C(3)-C(27)-C(28)	111.9 (5)	C(13)-C(35)-C(36)	109.3 (7)
C(2)-C(1)-C(20)	124.9 (5)	C(12)-C(11)-C(10)	126.0 (6)
N(21)-C(1)-C(20)	125.7 (5)	N(23)-C(11)-C(10)	125.2 (6)
N(21)-C(4)-C(5)	124.8 (5)	N(23)-C(14)-C(15)	125.3 (6)
C(3)-C(4)-C(5)	125.4 (5)	C(13)-C(14)-C(15)	126.3 (6)
C(5)-C(6)-C(7)	125.3 (5)	C(15)-C(16)-C(17)	125.7 (6)
C(5)-C(6)-N(22)	123.8 (5)	C(15)-C(16)-N(24)	123.7 (6)
C(6)-C(7)-C(29)	125.3 (5)	C(16)-C(17)-C(37)	126.6 (6)
C(7)-C(29)-C(30)	112.3 (6)	C(17)-C(37)-C(38)	109.9 (6)
C(8)-C(7)-C(29)	128.3 (6)	C(18)-C(17)-C(37)	126.6 (6)
C(7)-C(8)-C(31)	127.5 (6)	C(17)-C(18)-C(39)	127.5 (6)
C(8)-C(31)-C(32)	113.5 (6)	C(18)-C(39)-C(40)	111.6 (6)
C(9)-C(8)-C(31)	124.9 (6)	C(19)-C(18)-C(39)	125.6 (6)
C(10)-C(9)-C(8)	126.2 (6)	C(20)-C(19)-C(18)	125.0 (6)
C(10)-C(9)-N(22)	124.1 (6)	C(20)-C(19)-N(24)	124.7 (6)

[a] The number in parentheses is the estimated standard deviation.

activation energy of the process, determined as above,[19] is $\Delta G_c^{\ddagger} = 9.9 \pm 0.5$ kcal mol^{-1} at −65 °C.

UV–Visible Spectroscopic Study of Axial Ligation Equilibria. The formation of TPPTi(O_2) from TPPTiO and H_2O_2 in pyridine solution is conveniently monitored by UV–visible spectroscopy. A set of curves with well-defined isosbestic points, specifically in the Soret region at 440 nm, is obtained. This suggests that only two absorbing species are present, namely, TPPTiO and TPPTi(O_2) in equilibrium according to reaction 1. When a large excess of hydrogen peroxide is added

$$\mathrm{TPPTiO} + H_2O_2 \rightleftharpoons \mathrm{TPPTi}(O_2) + H_2O \qquad (1)$$

(H_2O_2/Ti > 10^3), a shoulder progressively grows on the Soret band, while the 440-nm isosbestic point shifts to shorter wavelengths. This indicates a second equilibrium, (2), following reaction 1 and involving TPPTi(O_2) and an unknown species X (vide infra).

Addition of H_2O_2 to a pyridine solution of TPPTi(O_2) prepared from an authentic sample also causes the appearance of a shoulder at 440 nm; an isosbestic point at 434 nm is then observed. Furthermore, addition of water or aqueous acid to a TPPTi(O_2) solution results in the same spectral changes. This shows that the unknown species X can be obtained from TPPTi(O_2) by several different reactions.

Finally, all of the above reactions are slow. Spectra recorded 10 min after addition of the reactants still change slowly with time and their reproducibility is poor. The kinetics are even slower for the OEPTiO/H_2O_2 system, which does not reach an equilibrium after 30 min of stirring at 30 °C.

Electrochemistry. The voltammetric curve of a dichloromethane solution of OEPTi(O_2) exhibits the four one-electron waves (two anodic and two cathodic) expected for the ring oxidation and reduction reactions.[21] An additional reduction step is observed, with a half-wave potential $E_{1/2} = -1.07$ V, just before the first ring reduction wave. The corresponding electrochemical reaction is irreversible in cyclic voltammetry. From the intensity of the limiting current, it is estimated that two electrons are involved; however, this stoichiometry cannot be confirmed by precise coulometric measurements at a controlled potential because of the closeness of the first ring reduction wave. The electrochemical behavior of TPPTi(O_2) is similar (Table XV).

Exhaustive electrolysis (about 2 F mol^{-1}) of a OEPTi(O_2) solution on a platinum-gauze cathode at a potential corresponding to the two-electron reduction step (−1.35 V) yields a solution whose electronic absorption spectrum and voltammogram are identical with those of OEPTiO.

Discussion

Formal Valency of the Dioxygen Ligand. Reaction of hydrogen peroxide with oxotitanium(IV) porphyrin complexes yields compounds which have an edge-bound dioxygen group. On the basis of the O–O separation and stretching frequency, this group is best described as a bidentate peroxide ligand similar to those found in the dioxygen adducts of Vaska-type complexes.[22] This class of triangular peroxide complexes is clearly distinct from the class of angular dioxygen adducts which are best described as superoxide complexes.[22] It is interesting to note that peroxide complexes can be obtained either by oxidative addition of dioxygen to a low-valent metal complex, e.g.

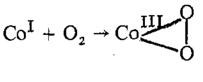

or by ligand exchange on a high-valent complex,[23] e.g.

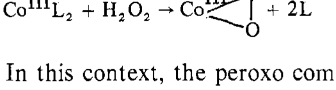

In this context, the peroxo complexes of titanium(IV) por-

Table XIV. NMR Data for $PTi(O_2)$ and PTiO

				Protons of R^1		Protons of R^2		Protons of R^3	
Compd	R^1	R^2	R^3	Mult/intens	δ, ppm	Mult/intens	δ, ppm	Mult/intens	δ, ppm
$OEPTi(O_2)$	H	C_2H_5	H	s/4	10.40	t/24	1.95	s/4	10.40
						q/15	4.13		
OEPTiO	H	C_2H_5	H	s/4	10.32	t/24	1.92	s/4	10.32
						q/16	4.03		
$TPPTi(O_2)$	C_6H_5	H	C_6H_5	m/12	7.82	s/8	9.18	m/12	7.82
				m/8	8.37			m/8	8.37
TPPTiO	C_6H_5	H	C_6H_5	m/12	7.81	s/8	9.07	m/12	7.81
				m/8	8.28			m/8	8.28
$MPOEPTi(O_2)$	H	C_2H_5	C_6H_5	s/1	10.35	t/6	1.23	m/3	7.22
						t/18	1.96		
				s/2	10.50	q/4	2.82	m/1	8.04
						q/12	4.12	m/1	8.52
MPOEPTiO	H	C_2H_5	C_6H_5	s/1	10.32	t/6	1.17	m/3	7.75
						t/18	1.95		
				s/2	10.41	q/4	2.78	m/2	Between 8.00 and 8.40
						q/12	4.13		

Table XV. Half-Wave Potentials[a] in Dichloromethane Solution

Compd	$(E_{1/2})^3_{\text{Red}}$	$(E_{1/2})^2_{\text{Red}}$	$(E_{1/2})^1_{\text{Red}}$	$(E_{1/2})^1_{\text{Ox}}$	$(E_{1/2})^2_{\text{Ox}}$	$(E_{1/2})^2_{\text{Red}} - (E_{1/2})^3_{\text{Red}}$	$(E_{1/2})^1_{\text{Ox}} - (E_{1/2})^2_{\text{Red}}$	$(E_{1/2})^2_{\text{Ox}} - (E_{1/2})^1_{\text{Ox}}$
$OEPTi(O_2)$	−1.61	−1.14	−1.07	+1.21	+1.67	0.47	2.35	0.46
$MPOEPTi(O_2)$	−1.62	−1.14	−1.09	+1.21	+1.58	0.48	2.35	0.37
$TPPTi(O_2)$	−1.37	−0.93	−0.83	+1.27	+1.53	0.44	2.20	0.26

[a] Potentials in volts relative to a $Ag/Ag_3I_4NBu_4$ reference electrode.[11] $(E_{1/2})^1_{\text{Red}}$ refers to the two-electron reduction of the peroxide ligand. Other $E_{1/2}$'s refer to ring redox reactions.

Table XVI. Bond Lengths (Å) and Angles (deg) for the $Ti(O_2)$ Unit in Some Titanium(IV) Peroxide Complexes

Compd	Ref	Ti-O(1)	Ti-O(2)	O(1)-O(2)	Ti-O(1)-O(2)	O(1)-O(2)-Ti	O(1)-Ti-O(2)
$[H_2OdipicTi(O_2)]_2O$	28a	1.872 (7)	1.905 (7)	1.45 (1)			45.2 (4)
$(H_2O)_2dipicTi(O_2)$	28b	1.834 (2)	1.858 (2)	1.464 (2)	67.50 (6)	67.78 (6)	46.72 (6)
(triclinic)	28e	1.842 (1)	1.862 (1)	1.469 (1)			
$(H_2O)_2dipicTi(O_2)$	28c	1.833 (1)		1.458 (2)	66.56 (6)		46.88 (6)
(orthorhombic)	28e	1.844		1.477			
$[F_2dipicTi(O_2)]^{2-}$	28b	1.846 (4)	1.861 (4)	1.463 (5)	67.3 (2)	66.2 (2)	46.5 (2)
$\{[NTATi(O_2)]_2O\}^{4-}$	28d	1.892 (2)	1.889 (2)	1.469 (2)	67.02 (6)	67.26 (6)	45.72 (6)
	28e	1.897	1.898	1.481			
$OEPTi(O_2)$	This work	1.827 (4)	1.822 (4)	1.445 (5)	66.5 (2)	66.9 (2)	46.7 (2)

phyrins are conceptually identical with the oxidative addition products of dioxygen and the hypothetical titanium(II) porphyrins.

Crystal Structure of $OEPTi(O_2)$. An important feature of the crystal structure of $OEPTi(O_2)$ is the position of the two oxygen atoms; they are bonded symmetrically on the titanium atom and eclipse perfectly the nitrogen atoms N(22) and N(24). Short distances between the oxygen atoms and the ethyl groups (Table XIII)[15] might suggest that the crystal packing is at the origin of this conformation. But this particular orientation of the peroxide group is also found in the *trans*-diperoxo complex of a molybdenum(VI) tetraarylporphyrin,[24] and a similar proximity of oxygen and nitrogens atoms is observed in two niobium(V) porphyrin complexes.[25,30] These observations lead us to consider that this structural arrangement is the preferential conformation of the isolated molecule. The dynamic NMR results (vide infra) are consistent with this interpretation.

The rather surprising preference of the oxygen atoms for the proximity of the nitrogen atoms of the macrocycle may be interpreted as the result of attractive and/or repulsive interactions. Simple considerations of symmetry show that the bonding interactions between the four nitrogen atoms, the titanium atom, and the two oxygen atoms are maximized when the two oxygen atoms eclipse two of the nitrogen atoms.[26] On the other hand, the significant difference between the mean values of the Ti–N(22) and Ti–N(24) bond lengths and those of the Ti–N(21) and Ti–N(23) distances, as already noted,[29] is a clue to a repulsion between O(1) and N(24) and between O(2) and N(22) or to a trans effect. Thus, the optimization of the bonding interactions imposing the proximity of the two oxygen atoms with two nitrogen atoms is moderated by the resulting repulsions.

The distances of the titanium atom from the mean plane of the four nitrogen atoms and from the mean plane of the macrocycle are significantly longer than those found for OEPTiO. This observation fits in with a repulsion effect between the oxygen and nitrogen atoms. The values of interatomic distances and angles of the $Ti(O_2)$ group in $OEPTi(O_2)$ are slightly shorter but otherwise close to those found by Schwarzenbach[28] for other titanium peroxide complexes (Table XVI).

Crystal Structure of OEPTiO. The observed Ti–O bond length and the Ti–N mean distance (1.613 (5) and 2.114 (6) Å) in OEPTiO in the monoclinic phase are essentially the same as those found in the orthorhombic form of OEPTiO[12] (1.667 (15) and 2.110 (9) Å), in titanyl α,γ-dimethyl-α,γ-dihydrooctaethylporphyrin[32] (respectively, 1.619 (4) and 2.110 (3) Å), and in vanadyl octaethylporphyrin[31] (1.620 (4) and 2.102 (6) Å). This last compound crystallized from toluene is isotypic to OEPTiO and $OEPTi(O_2)$. The Ti–N mean distance seems to be slightly shorter in OEPVO than in OEPTiO (2.102 Å compared to 2.114 Å).

Geometry of the Macrocycles. The values of the bond distances and angles in $OEPTi(O_2)$ (Tables VI and VII) and in OEPTiO (Tables VIII and IX) fall within the range of distances discussed by Hoard for other metalloporphyrins.[33] As expected, the pyrrole rings of OEPTiO and OEPTi(O_2) are planar within experimental error (Tables X and XI).[15] The mean values of the bond lengths and angles in the pyrrolic subunits of OEPTiO, OEPTi(O_2), and OEPVO are very similar. Only the bond length C_m–C_a in OEPTi(O_2) (1.381 (3) Å) is slightly shorter than the corresponding one in OEPTiO (1.391 (3) Å) and in OEPVO (1.387 (4) Å). Correlatively, the radius of the central hole Ct–N is shorter in OEPTi(O_2) (2.016 (5) Å) than in OEPTiO (2.040 (6) Å). Finally the plane defined by the four nitrogen atoms and the mean plane of the macrocycle are nearly parallel in OEPTiO and OEPTi(O_2): the distances between these planes (respectively, 0.054 and 0.037 Å) show the domed character of the porphyrin. Inspection of the angles between the normals to the pyrrole rings (Tables X and XI)[15] and examination of the departure of the atoms of the porphine core from the mean plane of the core show that the flatness of the macrocycle is better in OEPTi(O_2) than in OEPTiO.

Stereochemical Nonrigidity of the PTi(O_2) Complexes. A number of stereochemically nonrigid transition-metal chelates have been investigated by dynamic nuclear magnetic resonance (DNMR) during the last decade. Chelate complexes of Ti(IV) with β-diketones have been shown to undergo fast intramolecular rearrangement reactions for which various mechanistic pathways have been proposed.[34] From the DNMR behavior of OEPTi(O_2) and TPPTi(O_2) it can be concluded that these Ti(IV) macrocyclic complexes also exhibit stereochemical nonrigidity. The dynamic stereochemistry of these systems is easily interpreted in light of the crystal structure of OEPTi(O_2).

If the conformation of the OEPTi(O_2) molecule is the same in solution as in the solid state, then the two oxygen atoms of the peroxide group eclipse two opposite nitrogen atoms of the macrocycle. A magnetic perturbation of the carbon and hydrogen atoms belonging to the two eclipsed pyrrole rings with respect to those of the noneclipsed pyrrole rings is then expected. Indeed, the β pyrrole carbon atoms in OEPTi(O_2) exhibit two distinct resonances at low temperature. The fact that the signals of the ethyl carbon atoms, as well as those of the methylene protons, do not split or broaden at temperatures as low as −80 °C can be accounted for by the large distance of these nuclei from the magnetic perturbation. However, the reason the existence of two distinct sites for the peroxide group is not apparent in the DNMR signal of the α pyrrole carbons is not clear. Finally, the fact that the peaks of the meso carbon and hydrogen atoms do not split at low temperature precludes the hypothetical conformation in which the peroxide group would eclipse two meso carbon atoms.

The DNMR behavior of TPPTi(O_2) is interpreted in a similar manner, thus corroborating the hypothesis that the solid-state conformation observed for OEPTi(O_2) is also prevalent in solution for all peroxotitanium(IV) porphyrin complexes. The intramolecular nature of the averaging processes is supported by the independence of the coalescence temperature of the concentration and by the reversibility of the temperature-dependent spectral changes.

The rotation of the peroxide group at ambient temperature is similar to the exchange processes observed for coordinated olefins.[35] However, steric contributions to the rotation barrier which are found in several olefin complexes are absent in the planar macrocyclic titanium(IV) peroxide complexes. It thus appears that the rotation barrier measured for the peroxide group of PTi(O_2) complexes ($\Delta G_c^{\ddagger} = 10.3 \pm 0.5$ kcal mol^{-1}) has a purely electronic origin.[36]

TPPTiO + H_2O_2 Equilibria. Two successive equilibria, (1) and (2), are observed upon H_2O_2 addition to a TPPTiO solution. It is reasonable to assign the first reaction to the formation of the TPPTi(O_2) complex. Indeed, this complex can be isolated in these conditions; furthermore, identical absorption maxima are observed with an authentic solution of TPPTi(O_2).

Reaction 1 is slow at ambient temperature, making it difficult to determine the corresponding equilibrium constant. Despite numerous attempts, we have not been able to get consistent results.

The nature of the species X formed by the reaction of TPPTi(O_2) with hydrogen peroxide, water, or aqueous acid has not been elucidated. It seems that X is a metalloporphyrin, since it has an absorption peak near 440 nm which can be viewed as a Soret band. Furthermore, the high yield obtained in the preparation of TPPTi(O_2) indicates that the macrocycle is unaffected by H_2O_2 under the conditions described above. One can speculate that X is a *trans*-diperoxotitanium(IV) tetraphenylporphyrin complex; this coordination type has been demonstrated for a d^0 molybdenum(VI) complex.[24] Such a complex could be made either by coordination of a second peroxide group in trans position on TPPTi(O_2) according to reaction 2 or by disproportionation of TPPTi(O_2) in the presence of water according to reaction 3. Equilibria 1–3

$$\mathrm{TPPTi(O_2) + H_2O_2 \rightleftharpoons TPPTi(O_2)_2{}^{2-} + 2H^+} \tag{2}$$

$$\mathrm{2TPPTi(O_2) + H_2O \rightleftharpoons TPPTi(O_2)_2{}^{2-} + TPPTiO + 2H^+} \tag{3}$$

could conceivably be catalyzed by acid. Other interpretations are conceivable, however, and the elucidation of the nature of species X will require further experiments.

The least soluble species in this system is TPPTi(O_2), which is obtained by addition of water to the reaction mixture. Equilibria 2 and 3 are presumably driven to the left by TPPTi(O_2) precipitation.

Electrochemistry. Peroxotitanium(IV) porphyrin complexes can be reduced electrochemically to the corresponding oxotitanium(IV) complexes in a two-electron irreversible process. The nature of the product indicates that reduction occurs neither at the metal ion nor at the porphyrin ring but rather at the axial peroxide ligand according to reaction 4. This

$$\mathrm{PTi^{IV}(O_2) + 2e^- \rightarrow [PTi^{IV}O_2]^{2-}} \tag{4}$$

$$\mathrm{[PTi^{IV}O_2]^{2-} + H_2O \rightarrow PTi^{IV}O + 2HO^-} \tag{5}$$

reductive cleavage of the O–O bond generates two oxide ions, one of which is coordinated to the Ti(IV) ion. The other, highly basic oxide ion probably reacts with a proton donor, e.g., residual water, background electrolyte, or solvent, according to reaction 5. The occurrence of this follow-up chemical reaction accounts for the irreversiblity of the overall process.

The above mechanism is very different from the one which has been proposed for the electrochemical reduction of $(\mathrm{dppe})_2\mathrm{Ir}(O_2)^+$, a Vaska-type dioxygen complex.[9,38] In that case, a one-electron reduction step results in the liberation of superoxide ion according to reaction 6. Very few investi-

$$\mathrm{(dppe)_2Ir(O_2)^+ + e^- \rightarrow (dppe)_2Ir^+ + O_2{}^{-}\cdot} \tag{6}$$

gations of the redox properties of dioxygen complexes have been reported, and the factors which govern their electrochemical behavior are unknown. Further work will be necessary to elucidate the causes of the difference in behavior noted above.

The half-wave potentials for the peroxide group reduction in OEPTi(O_2) and TPPTi(O_2) differ by 240 mV (Table XVI). This difference is close to that observed for a ring reduction in OEP and TPP complexes.[39] It thus appears that the peroxide group feels the electronic effects of the macrocycle substituents. One can speculate that these electronic effects are transmitted through the interaction of a ring $e_g(\pi^*)$ orbital and the peroxide $3\sigma_u{}^*$ orbital.

Conclusion

Peroxotitanium(IV) porphyrin complexes provide unequivocal evidence that coordination of a dioxygen group in an edge-bound fashion to a metalloporphyrin is possible. In these compounds, a preferred conformation in which the two oxygen atoms eclipse two opposite nitrogen atoms of the porphyrin is adopted in the solid state as well as in solution. In the latter case, however, the peroxide ligand undergoes ready exchange between the two possible preferred sites. The coordinated peroxide group exhibits two remarkable properties: it can be reduced to the lowest oxidation state of oxygen O(−II), and it feels the electronic effects of the macrocycle substituents. Such properties may have important implications for the biologically occurring iron porphyrin complexes if iron peroxide complexes exist in some hemoproteins. We are currently investigating the reactivity of $PTi(O_2)$ complexes to test possible analogies with the oxygenases. We are also trying to find new synthetic routes to $PTi(O_2)$ using dioxygen rather than hydrogen peroxide.[40]

Acknowledgment. We thank Henri Reutenauer of the Laboratoire Grenoblois de Rêsonance Magnêtique Nucléaire â Haute Rêsolution for his help in recording the DNMR spectra. We are indebted to Yves Ellinger of the Centre d'Etudes Nucléaires de Grenoble for helpful discussions.

Registry No. $OEPTi(O_2)$, 60217-35-8; OEPTiO, 25087-66-5; $TPPTi(O_2)$, 65651-28-7; TPPTiO, 58384-89-7; $MPOEPTi(O_2)$, 65651-27-6; MPOEPTiO, 60193-54-6; ^{13}C, 14762-74-4.

Supplementary Material Available: Listings of structure factor amplitudes and Tables III, V, and X–XIII showing positional parameters for H atoms, least-squares planes, and intermolecular contact distances (72 pages). Ordering information is given on any current masthead page.

References and Notes

(1) (a) Université de Dijon. (b) Centre d'Etudes Nucléaires de Grenoble. (c) Université de Nancy.

(2) (a) F. Basolo, B. M. Hoffman, and J. A. Ibers, *Acc. Chem. Res.*, **8**, 384 (1975), and references therein; (b) J. H. Fuhrhop, *Angew. Chem., Int. Ed. Engl.*, **15**, 648 (1976), and references therein; (c) J. P. Collman, *Acc. Chem. Res.*, **10**, 265 (1977), and references therein.

(3) J. P. Collman, R. R. Gagnê, C. A. Reed, T. R. Halbert, G. Lang, and W. T. Robinson, *J. Am. Chem. Soc.*, **97**, 1427 (1975).

(4) (a) F. A. Walker, *J. Am. Chem. Soc.*, **92**, 4235 (1970); (b) D. V. Stynes, H. C. Stynes, B. R. James, and J. A. Ibers, *ibid.*, **95**, 1796 (1973); (c) B. M. Hoffman and D. H. Petering, *Proc. Natl. Acad. Sci. U.S.A.*, **67**, 637 (1970).

(5) S. T. Cheung, C. J. Grimes, J. Wong, and C. A. Reed, *J. Am. Chem. Soc.*, **98**, 5028 (1976).

(6) (a) B. Gonzalez, J. Kouba, S. Yee, C. A. Reed, J. Kirner, and W. R. Scheidt, *J. Am. Chem. Soc.*, **97**, 3247 (1975); (b) B. M. Hoffman, C. J. Weschler, and F. Basolo, *ibid.*, **98**, 5473 (1976).

(7) (a) J. P. Collman, J. I. Brauman, T. R. Halbert, and K. S. Suslick, *Proc. Natl. Acad. Sci. U.S.A.*, **73**, 3333 (1976); (b) C. A. Reed and S. K. Cheung, *ibid.*, **74**, 1780 (1977).

(8) P. Fournari, R. Guilard, M. Fontesse, J.-M. Latour, and J.-C. Marchon, *J. Organomet. Chem.*, **110**, 205 (1976).

(9) The following abbreviations are used throughout this article: OEP, octaethylporphinato; TPP, tetraphenylporphinato; MPOEP, *meso*-phenyloctaethylporphinato; P, porphinato; dppe, bis(diphenylphosphino)ethane.

(10) R. Guilard, M. Fontesse, P. Fournari, C. Lecomte, and J. Protas, *J. Chem. Soc., Chem. Commun.*, 161 (1976).

(11) D. Coutagne, *Bull. Soc. Chim. Fr.*, 1940 (1971).

(12) C. Lecomte, J. Protas, and R. Guilard, *C. R. Hebd. Seances Acad. Sci., Ser. C*, **281**, 921 (1975).

(13) C. Germain, P. Main, and M. M. Woolfson, *Acta Crystallogr., Sect. A*, **27**, 328 (1971).

(14) W. R. Busing, K. O. Martin, and H. A. Levy, USAEC Report ORNL-TM 305, Oak Ridge National Laboratory, Oak Ridge, Tenn., 1962.

(15) Supplementary material.

(16) A. H. Jackson, G. W. Kenner, K. M. Smith, R. T. Aplin, H. Budzikiewicz, and C. Djerassi, *Tetrahedron*, **21**, 2913 (1965).

(17) (a) W. P. Griffith, *J. Chem. Soc.*, 5248 (1964); (b) E. Wendling, *Bull. Soc. Chim. Fr.*, 16 (1967); (c) J. Mühleback, K. Müller, and G. Schwarzenbach, *Inorg. Chem.*, **9**, 2381 (1970).

(18) S. S. Eaton and G. R. Eaton, *J. Am. Chem. Soc.*, **97**, 3660 (1975).

(19) H. Kessler, *Angew. Chem., Int. Ed. Engl.*, **9**, 219 (1970).

(20) (a) R. J. Abraham and K. M. Smith, *Tetrahedron Lett.*, **36**, 3335 (1971); (b) R. J. Abraham, G. H. Barnett, and K. M. Smith, *J. Chem. Soc., Perkin Trans. 1*, 2142 (1973); (c) C. A. Busby and D. Dolphin, *J. Magn. Reson.*, **23**, 211 (1976).

(21) J. H. Fuhrhop, K. M. Kadish, and D. G. Davis, *J. Am. Chem. Soc.*, **95**, 5140 (1973).

(22) L. Vaska, *Acc. Chem. Res.*, **9**, 175 (1976).

(23) B. Bosnich, H. Boucher, and C. Marshall, *Inorg. Chem.*, **15**, 634 (1976).

(24) B. Chevrier, T. Diebold, and R. Weiss, *Inorg. Chim. Acta*, **19**, L57 (1976).

(25) (a) C. Lecomte, J. Protas, and R. Guilard, *C. R. Hebd. Seances Acad. Sci., Ser. C*, **283**, 397 (1976); (b) J. F. Johnson and W. R. Scheidt, *J. Am. Chem. Soc.*, **99**, 294 (1977).

(26) Such considerations are based on a symmetry analysis of an orbital model similar to that described by Hoffmann et al.:[27] Y. Ellinger, J. M. Latour, J. C. Marchon, and R. Subra, *Inorg. Chem.*, in press.

(27) R. Hoffmann, M. M. L. Chen, and D. L. Thorn, *Inorg. Chem.*, **16**, 103 (1977).

(28) (a) D. Schwarzenbach, *Inorg. Chem.*, **9**, 2391 (1970); (b) D. Schwarzenbach, *Helv. Chim. Acta*, **55**, 2990 (1972); (c) H. Manohar and D. Schwarzenbach, *ibid.*, **57**, 1086 (1974); (d) D. Schwarzenbach and K. Girgis, *ibid.*, **58**, 2391 (1975); (e) D. Schwarzenbach, *Z. Kristallogr., Kristallgeom., Kristallphys., Kristallchem.*, **143**, 429 (1976).

(29) A similar, more important effect was observed in the acetatooxo complex of niobium(V) tetraphenylporphyrin.[30] However, the Ti–N mean distance in $OEPTi(O_2)$ (2.111 Å) is close to those found in OEPTiO (vide supra) and OEPVO.[31]

(30) C. Lecomte, J. Protas, R. Guilard, B. Fliniaux, and P. Fournari, *J. Chem. Soc., Chem. Commun.*, 434 (1976).

(31) F. S. Molinaro and J. A. Ibers, *Inorg. Chem.*, **15**, 2278 (1976).

(32) P. N. Dwyer, L. Puppe, J. W. Buchler, and W. R. Scheidt, *Inorg. Chem.*, **14**, 1782 (1975).

(33) J. L. Hoard in "Porphyrins and Metalloporphyrins", K. M. Smith, Ed., Elsevier, Amsterdam, 1976.

(34) R. H. Holm in "Dynamic Nuclear Magnetic Resonance Spectroscopy", L. M. Jackman and F. A. Cotton, Ed., Academic Press, New York, N.Y., 1975.

(35) F. A. Cotton in "Dynamic Nuclear Magnetic Resonance Spectroscopy", L. M. Jackman and F. A. Cotton, Ed., Academic Press, New York, N.Y., 1975.

(36) Ab initio calculation of the barrier to rotation of the peroxide group in an unsubstituted $PTi(O_2)$ complex gives a value of about 5 kcal mol^{-1}.[37]

(37) M. M. Rohmer, M. Barry, A. Dedieu, and A. Veillard, *Int. J. Quantum Chem., Quantum Biol. Symp.*, **No. 4**, 337 (1977).

(38) B. K. Teo, A. P. Ginsberg, and J. C. Calabrese, *J. Am. Chem. Soc.*, **98**, 3027 (1976).

(39) J. H. Fuhrhop, *Struct. Bonding (Berlin)*, **18**, 1 (1974).

(40) Oxygenation of a fluoro complex of titanium(III) tetraphenylporphyrin affords a 1:1 mixture of $TPPTi(O_2)$ and $TPPTiF_2$. See M. Nakajima, J.-M. Latour, and J.-C. Marchon, *J. Chem. Soc., Chem. Commun.*, 763 (1977).